



e-ISSN:2582 - 7219



INTERNATIONAL JOURNAL OF MULTIDISCIPLINARY RESEARCH IN SCIENCE, ENGINEERING AND TECHNOLOGY

Volume 4, Issue 12, December 2021



INTERNATIONAL
STANDARD
SERIAL
NUMBER
INDIA

Impact Factor: 5.928



9710 583 466



9710 583 466



ijmrset@gmail.com



www.ijmrset.com



X-Ray Photoelectron Spectroscopy of $\text{FeSe}_x\text{Te}_{1-x}$ Superconducting Compounds

Harish Kumar Sublania¹, Ram Bilas Meena², Deepmala Meena¹

¹Department of Physics, Government College, Kota, Rajasthan, India

²Department of Chemistry, Government College, Kota, Rajasthan, India

ABSTRACT: In this work electronic structure property of Fe-chalcogen based compounds are studied to confirm the nature of superconductivity as well as the reason behind the superconducting properties. The various highly polarized X-ray Photoelectron Spectroscopy (XPS) spectra were measured at the synchrotron radiation beamline at ELLETRA, Italy are analyzed and compared to study the mechanism responsible in these compounds. From our analysis we have observed that the doping shift the XPS spectra to the higher energy side, which may be due to the changes the coordination geometry of various bonds. With Te/Se doping the coulomb interaction is reported to enhance with the increased electron doping between the layers which is also due to the decreased distance between FeSe/FeTe layers and decreases the intensity of the $\text{FeSe}_{0.5}\text{Te}_{0.5}$ sample.

KEYWORDS: Fe-chalcogen superconductors, XPS, Charge carries, Electronic structure.

I. INTRODUCTION

The discovery of superconductivity in $\text{LaFeAsO}_{1-x}\text{F}_x$ [1] was a surprising thing because in the most cases, iron element is a killer of superconductivity due to its strong magnetic moment. The iron-based superconductors have been formed a new family in the field of high T_c superconductivity [1, 2]. In the FeAs based compounds, several structures have been found, including the so called 1111 phase (LnFeAs , AeFeAsF where Ln= rare earth elements, Ae= alkaline) with maximum T_c at about 56K [3,4], 122 phase (AeFe_2As_2) with T_c 38K [5,6,7], 111 phase LiFeAs , and 11 phase (FeSe) [8] at about 8K and increase in T_c to 27 with the application of 1.45Gpa has been reported for FeSe [9,10]. In the wide range of iron-based superconductors, FeSe system remains of considerable interest because it is the foundation of which more complicated layered structures are formed. The PbO type structure of FeSe composed of planar layer of Fe_2Se_2 similar to the Fe_2As_2 layers of FeAs family of superconductors. In FeAs family, there is an addition layer either of LnO in the LnOFeAs series, Ae layer in the AeFe_2As_2 or Li (Na) layer in the Li(Na)FeAs compounds. In the study of magnetic order, physical properties, and electronic structure FeSe is preferable material over FeAs compounds because it has only one type of planes layer [11].

$\text{FeSe}_{1-x}\text{Te}_x$ has only a continuous stacking of tetrahedral FeSe(Te)_4 layers without any sandwiching spacer. The stoichiometric compounds are very close to spin density wave (SDW) instability and the appearance of antiferromagnetic ground state [12, 13]. The superconductivity temperature increase with T_c doping reaches a maximum at about 50% substitution and then decreases with more Te doping [14]. Tellurium (Te) substitution has been studied [15] and maximum superconducting transition temperature of 15.2K was measured for $\text{FeSe}_{0.5}\text{Te}_{0.5}$ [16]. The transition temperature in very recently discovered ternary iron selenides $\text{AyFe}_{2-x}\text{Se}_2$ ($A = \text{K, Rb, Cs...}$) [17-20] is very high at ambient pressure [8], which is surprising because the system is thought to heavily electron doped. In this paper, we present the results of XPS measurement on FeTe , FeSe , and $\text{FeSe}_{0.5}\text{Te}_{0.5}$ system and to estimate the contribution from different components Gaussians are fit. X-ray photoelectron spectroscopy is a powerful tool in probing the electronic states near Fermi level in the transition metal and hence we employed this technique to explain the behavior of these samples. The results a represented in the direction of all possible hybridization, shifting of density of states and charge carrier localization in these compounds.

II. EXPERIMENTAL DETAILS

The X-ray Photoelectron Spectroscopic (XPS) was made on these samples at the BACH beamline of the highly polarized synchrotron radiation beam at Elettra, Trieste, Italy. The polycrystalline samples of $\text{FeSe}_{0.5}\text{Te}_{0.5}$ were used for measurements, performed at room temperature. The samples were cleaned *insitu* using the hard scraping in the UHV conditions at the pressure 5×10^{-10} mbar. For a better signal to noise ratio and to ensure the reproducibility of the data, several scans were collected for different measurement. The core level energy scale was calibrated using the $\text{Au } 4f_{7/2}$



binding energy set at 83.9 eV. The XPS spectra were recorded for the Fe 2p, Se 3d and Te 3d core level binding energies spectrum. In this paper we have probed the electronic and chemical structure of FeSe_{0.5}Te_{0.5} sample using these core level spectra using the fitting of Gaussians in various spectral peaks. The measured kinetic electron energies E_{kin} are converted into the electron binding energies E_b by the classical formula:

$$E_{kin} = E_{ph} - E_b$$

With the incident photon energy E_{ph} .

III. RESULTS AND DISCUSSION Fe 2p XPS Spectra

The transition- metal Fe 2p core- level spectra for FeSe_{0.5}Te_{0.5}FeTe, and FeSe samples is shown in figure 1. The Fe 2p photoemission spectra is a two component peak, one is attributed its presence due to Fe 2p_{3/2} and another peak is attributed due to Fe 2p_{1/2}. This splitting is aroused due to spin orbit coupling in the final state. There will be coupling between the unpaired spin and orbital angular momentum mainly due to the non-zero orbital angular momentum of p-orbitals. By taking the idea from Y. Zhang et al [21] we can say that present coupling of course has no any evidence with s level, but has seen with p, d, and f core levels which all show the features of spin orbital doublets. The main peaks on the low binding energy side of 2p level are separated by 13eV energy from the satellite peak which seen on the high energy side[21].

The Gaussians are fit to estimate the contribution of various factors in these spectra the graph after fitting are shown by solid line with circles, which shows a complete agreement with the experimental data. The various Gaussians contributing in the fitting are shown by dashed line. After the fitting one can see that a Fe2p_{3/2} line is decomposed into three peaks. The first Gaussian at 706.41eV may be attributed its presence due to pure Fe metal peak; other two Gaussians arise due to the contamination present at the surface. The second Gaussian at 708.00eV is surface peak, and its origin may be attributed to FeO (Fe²⁺) and the third Gaussian at 712.00eV is satellite peak, which may be ascribed its presence due to possible hybridization with Se 4p/Te5p.

The areas of the Gaussian peaks are shown in the table 1, here for our all present samples. From the many research on Fe-Ch superconductors we can say that the above changes may be due to the structural changes due to Se/Te doping. The relative area of the Fe 2p_{1/2} peak decreases as we go from FeTe system to FeSe_{0.5}Te_{0.5} system in the opposite scenes of intensity of the peaks, the FeSe_{0.5}Te_{0.5} has highest intense peak but lowest relative area of same peak. It may be concluded that the relative area of the Fe 2p_{1/2} peak is decreased with doping (Seatom).

Se 3d XPS spectra:-

The Se 3d core level spectra of FeSe_{0.5}Te_{0.5} and FeSe samples are shown in figure 2. For the FeSe sample the Se 3d core level spectrum peak is a single component peak and for the FeSe_{0.5}Te_{0.5} sample the peak is two component peaks. In this spectra the Se 3d_{5/2} (52.98eV) and Se 3d_{3/2} (53.74 eV) can be observed, which arise due to spin orbit coupling effects in final state, which may be ascribed their presence due to hybridization with Te. The Se two peaks have the small energy gap, so it is concluded that the spin- orbit splitting has very weak significant for Se 3d core levels [21]. The Gaussians are fitted to estimate the contribution from different components and the lower energy Gaussian peak may be existed due to the contribution of pure Se only and higher energy Gaussian peak may be attributed due to the hybridization with Fe 3d. One extra Gaussian peak in FeSe_{0.5}Te_{0.5} spectra are attributed due to ion state of Te corresponding to Fe-Te band. The Se 3d peaks appear to have lower intensity after substitution of Te content. It is mainly due to decreased number of Se 4p states by replacing some concentration of Se with Te near the Fermi level.

From the table 2, we can see the change in the spectral weight of Gaussian peaks for the FeSe and FeSe_{0.5}Te_{0.5} samples. From the spectra we can see that one peak having A₃ is absent in FeSe sample because it may have its contribution due to Te hybridization which one clearly seen in FeSe_{0.5}Te_{0.5} sample after Te doping and the area of other peaks decreases upon Te doping.

Te 3d XPS Spectra:

The characteristic XPS spectra for Tellurium (Te) for the FeTe and FeSe_{0.5}Te_{0.5} samples, the two peak spectra represents split components Te 3d_{5/2} and Te 3d_{3/2}, it shows that there is also a spin orbital coupling effect in the final state. The 3d_{5/2} and 3d_{3/2} core level spectrum of Te for FeSe_{0.5}Te_{0.5} sample is deconvoluted into three Gaussian peaks. The first Gaussian peak corresponding to pure Te metal while second peak is surface peak and third may be appeared due to the hybridization with Se/Fe. The core spectrum of FeSe_{0.5}Te_{0.5} is slightly shifted to higher energy side and decreases the intensity of peak as compared with FeTe sample. This shifting might be due to the decreases of bond length of Fe-Fe and Fe-Te after Se substitution. The intensity of Te 3d spectra for FeSe_{0.5}Te_{0.5} sample is attributed to the decreases of the Te 3d electrons near the Fermi level after replacing with Se element [28,29]. The spectral weight of the above fitted Gaussians in Te 3d spectra of FeTe and FeSe_{0.5}Te_{0.5} samples.



It can be seen from the figure that the area of peak A_1 decreases with Se doping but area of peaks A_2 and A_3 increases. Here we calculated the relative area of Te $3d_{3/2}$ peak and it can be seen that this relative area increases and broadening in the Te $3d$ Peaks with Se doping in the system.

L. Simonelli et al [22] studied the effect of high- temperature annealing manifested that the compressed phase with a lower-spin Fe^{2+} state is directly related to the high T_c superconductivity in the system. So we can say that this Fe^{2+} states also very important state for superconducting system. We can see from some reported results that some system like LaOFeP [23], LaOFeAs [24], and CaFe₂As₂ [25] in Fe $2p$ XPS spectra there have been no third peak i.e satellite peak (712.00eV) but pure Fe metal peak is same in these studies also. The presence of pure metal peak and absence of satellite peak in the above samples may be due to the charge- carrier localization induced by excess Fe at the $2c$ site [26]. After going to literature of the x ray studies, we can observe that there is existence of the itinerant character of Fe $3d$ electronic state which may be caused by hybridization of the Fe $3d$ state with the Se $4p$ /Te $5p$ states [25]. The removal of electron from the $2p$ orbital by photo- ionization may lead to the hybridization between the $3d$ shells with $2p$ electrons. Similarly the explanation regarding various Gaussians fitted to Fe $2p_{1/2}$ lines into three components can be ascribed as for the Fe $2p_{3/2}$ peak for FeSe_{0.5}Te_{0.5} Sample [21]. By taking the some clue from Joseph et al [27], it can be observed that the peak intensity of FeSe_{0.5}Te_{0.5} sample is increased and shifted to higher energy side, which may be due to the strengthening of the hybridization between Fe $2p$ and Se $4p$ and increase in the valence states. The increment in the valence is an indication of the change in the coordination geometry and increase in the number of $4p$ holes.

The inner core electronic configuration of the initial state of Fe is [Ar] $(3d)^6(4s)^2$ with sub-shells completely filled. The removal of an electron from the $2p$ orbital by photo- ionization may lead to the coupling between the $3d$ shells with the $2p$ electrons [21]. Hence we can also say that with Tellurium doping, the electron density in the conduction layer increases. As Te doping, the distance between FeSe layers prominently decreases which indicated that the electron doping enhances coulomb interaction and polarization between the layers. So we can conclude that AFM order and structural phase transition is suppressed by Te doping up to 50% while superconductivity enhanced [15].

IV. CONCLUSION

This investigation discussed the XPS for various core level spectra on Fe $2p$, Se $3d$, and Te $3d$ for the FeSe, FeTe and FeSe_{0.5}Te_{0.5} system. In X- ray photoelectron spectroscopy studies of present samples revealed well defined positions for Iron (Fe), Selenium (Se) and Tellurium (Te) but along with sufficient hybridization. The comparison between various features arises due to hybridization is explained to understand the electronic structure of these samples. In Fe $2p$ XPS, it has been found that main peaks and satellite peaks shift to high energy side with higher intensity, this may be ascribed due to the chemicals and structural changes in the lattice i.e Fe-Fe and Fe-Te/Se bond and strengthen the hybridization with Se/Te doping. From Se $3d$ and Te $3d$ XPS, we have also found that with Te/Se doping the coulomb interaction may be enhanced with the increased electron doping between the layers which is also due to the decreased distance between FeSe/FeTe layers and decreases the intensity of the FeSe_{0.5}Te_{0.5} sample. The AFM order and structural phase transition is also suppressed by Te doping up to 50% while superconductivity enhanced with the changes in local geometry around the Se and Te atoms. It is concluded that the doping affects the spectra and shift to the higher energy side may be due to the changes the bonds between these three Fe, Se, and Te element i.e change the coordination geometry.

REFERENCES

1. Y. Kamihara, T. Watanabe, M. Hirano, H. Hosono, J. Am. Chem. Soc. **130** (2008) 3296.
2. H. H. Wen, J. Adv. Mat. **20**(2008) 3764.
3. P. Cheng, B. Shen, G. Mu, X. Zhu, F. Han, B. Zeng, H. H. Wen, EPL **85** (2009) 67003.
4. X. Zhu, F. Han, P. Cheng, G. Mu, B. Shen, H. H. Wen, EPL **85**(2009)17011.
5. S. Sefet, R. Jin, M. A. Mchuine, B. C. Sales, D. J. Singh, D. Mandrus, Phys. Rev. Lett. **101**(2008)117009.
6. M. Rotter, M. Tegel, D. Johrendt, I. Schellenberg, W. Hermes, R. Pottgen, Phys. Rev. **B 78** (2008)0250503.
7. X.C.Wang,Q.Q.Liu,Y.X.Lv,W.B.Gao,L.X.Yang,R.C.Yu,F.Y.Li,C. Q. Jin, J. Sol. State Commu; **148** (2008) 538.
8. F. C. Hsu, J. Y. Lu, K. W. Yen, T. K. Chen, T. W. Huang, P. M. Wu, Y. C. Lee, Yi L. Huang, Y. Y. Chu, D. C. Yan, M. K. Wu, J. Proc. Nat. Acad. Sci. **105** (2008)14262.
9. E.Z.Kurmaev,J.A.McLeod,N.A.Skorikov,L.D.Finkelstein,A.Moewes, 12. M.A. Korotin, Y. A. Izyumov, Y. L. Xie, G. Wu, X. H. Chen, J. Phys. Condens. Matt. **21** (2009) 435702.



10. N. L. Saini, Y. Wakisaka, B. Joseph, A. Iadecola, S. Delala, P. Srivastava, E. Magnano, M. Malvestuto, Y. Mizuguchi, Y. Takano, T. Mizokawa, K. B. Garg, Phys. Rev. **B 83** (2011)052502.
11. F.C.Hsu,J.Y.Luo,K.W.Yeh,T.K.Chen,T.W.Huang,P.M.Wu,Y.C.Lee, Y. L. Huang, Y.Y. Chu, D.C. Yan, M. K. Wu, J. Proc. Natl. Acad. Sci. USA **105**(2008) 14262.
12. S. Medvedev, T. M. Mcqueen, I. A. Troyan, T. Palasyuk, M. I. Erements, R. J. Cava, S. Naghavi, F. Casper, V. Ksenofontov, G. Wortmann, C. Felser, Nature Mater. **8** (2009)630.
13. Ricci, B. Joseph, N. Poccia, W. Xu, D. Chen, W. S. Chu, Z. Y. Wu, A. Marcelli, N. L. Saini, A. Bianconi, J. Supercond. Sci. Technol. **23** (2010)052003.
14. W. Bao, Y. Qiu, Q. Huang, M. A. Green, P. Zajdel, M. R. Fitzsimmons, M. Zhernenkov,S.Chang,M.Fang,B.Qian,E.K.Vehstedt,J.Yang,H.M.Pham, L. Spinu, Z. Q. Mao, Phys. Rev. Lett. **102** (2009) 247001.
15. K.W. Yeh, T.W. Huang, Y. L. Huang, T. K. Chen, F. C. Hsu, P. M. Wu, Y. C. Lee, Y. Y. Chu, C. L. Chen, J. Y. Luo, J. Europhys. Lett. **84** (2008)37002.
16. G. Tsoi, A. K. Stemshorn, Y. K. Vohra, P. M. Wu, F. C. Hsu, Y. L. Huang, M. K. Wu, K. W. Yeh, S. T. Weir, J. Phys. Conden. Matt. **21** (2009)232201.
17. Y. Mizuguchi, H. Takeya, Y. Kawasaki, T. Ozaki, S. Tsuda, T. Yamaguchi, Y. Takano. Appl. Phys. Lett. **98** (2011)042511.
18. D. M. Wang, J. B. He, T. L. Xia, G. F. Chen, Phys. Rev. **B 83** (2011)132502.
19. F. Wang, J. J. Ying, Y. J. Yan, R. H. Liu, X. G. Luo, Z. Y. Li, X. F. Wang, M. Zhang, G. J. Ye, P. Cheng, Z. J. Xiang, X. H. Chen, Phys. Rev. **B 83** (2011) 060512(R).
20. M. Fang, H. Wang, C. Dong, Z. Li, C. Feng, J. Chen, H. Q. Yuan, Europhys.Lett. **94** (2011) 27009.
21. Y. Zhang, Y. L. Chen, Y. J. Cui, C. H. Cheng, H. Zhang, Y. Zhao, J. Supercond. Sci. Technol. **22** (2009)015007.
- L. Simonelli, N. L. Saini, M. M. Sala, Y. Mizuguchi, Y. Takano, H. Takeya, T. Mizokawa, G. Monaco, Phys. Rev. **B 85** (2012)224510.
22. D. H. Liu, M. Yi, S. K. Mo, A. S. Erickson, A. Analytis, J. H. Chu, D. J. Singh, Z. Hussain, T. H. Gebballe, I. R. Fisher and Z. X. Shen, Nature **455** (2008)81.
23. W. Malaeb, T. Yoshida and T. Kataoka, J. Phys. Soc. Japan **77** (2008)093714.
- Yamasaki, Y. Matsui, S. imada, K. Takase, H. Azuma, T. Muro, Y. Kato, A. Sekiyama, S. Suga, A. Higashiya, M. Yabashi, K. Tamasaku, T. Ishikawa, K. terashima, H. Kobori, A. Sugimura, N. Umeyama, H. Sato, Y. Hara, N. Miyakawa, S. I. Ikeda, J. of Phy.: Conference Series **391** (2012)012141.
24. T.J.Liu,X.Ke,B.Qian,J.Hu.,D.Fobes,E.K.Vehstedt,H.Pham,J.H.Yang,M. H. Fang, L. Spinu, P. Schiffer, Y. Liu and Z. Q. Mao, Phys. Rev. **B 80**, 174509 (2009).
25. B. Joseph, A. Ladecola, L. Simonelli, Y. Mizuguchi, Y. Takano, T. Mizokawa, N. L. Saini, J. Phys. Conden. Matt. **22** (2010) 485702-485706.
26. R. S. Kumar, Y. Zhang, S. Sinogeikin, Y. Xiao, S. Kumar, P. Chow, A. L. Cornelius, C. Chen, J. Phys. Chem. **B 114** (2010)12597.
27. G. Garbarino, A. Sow, P. Lejay, A. Sulpice, P. Toulemonde, M. Mezouar, M. N. Regueiro, Europhys. Lett. **86** (2009)27001.

Table

Area →	A ₁	A ₂	A ₃	Relative area of Fe 2p _{1/2} peak
FeTe	2.6339	3.0537	2.7708	0.51266
FeSe	3.5869	3.5296	4.3517	0.54817
FeSe _{0.5} Te _{0.5}	4.07813	6.71871	5.2084	0.56086

Table 1: Area of peaks for Fe 2p XPS on FeTe, FeSe, and FeSe_{0.5}Te_{0.5} samples



Area →	A ₁	A ₂	A ₃	Relative area of Se/Te 3d peak
FeSe	153.68	67.131	-	-
FeSe _{0.5} Te _{0.5}	98.72727	42.01454	35.10364	0.19963

Table 2: Area of peaks for Se 3d XPS on FeSe and FeSe_{0.5}Te_{0.5} samples.

Area →	A ₁	A ₂	A ₃	Relative area of Te 3d _{3/2} peak
FeTe	7.6940	4.5533	3.0719	0.37178
FeSe _{0.5} Te _{0.5}	6.9633	6.6183	3.7662	0.48729

Table 3: Area of peaks for Te 3d XPS on FeTe and FeSe_{0.5}Te_{0.5} samples.

Figure

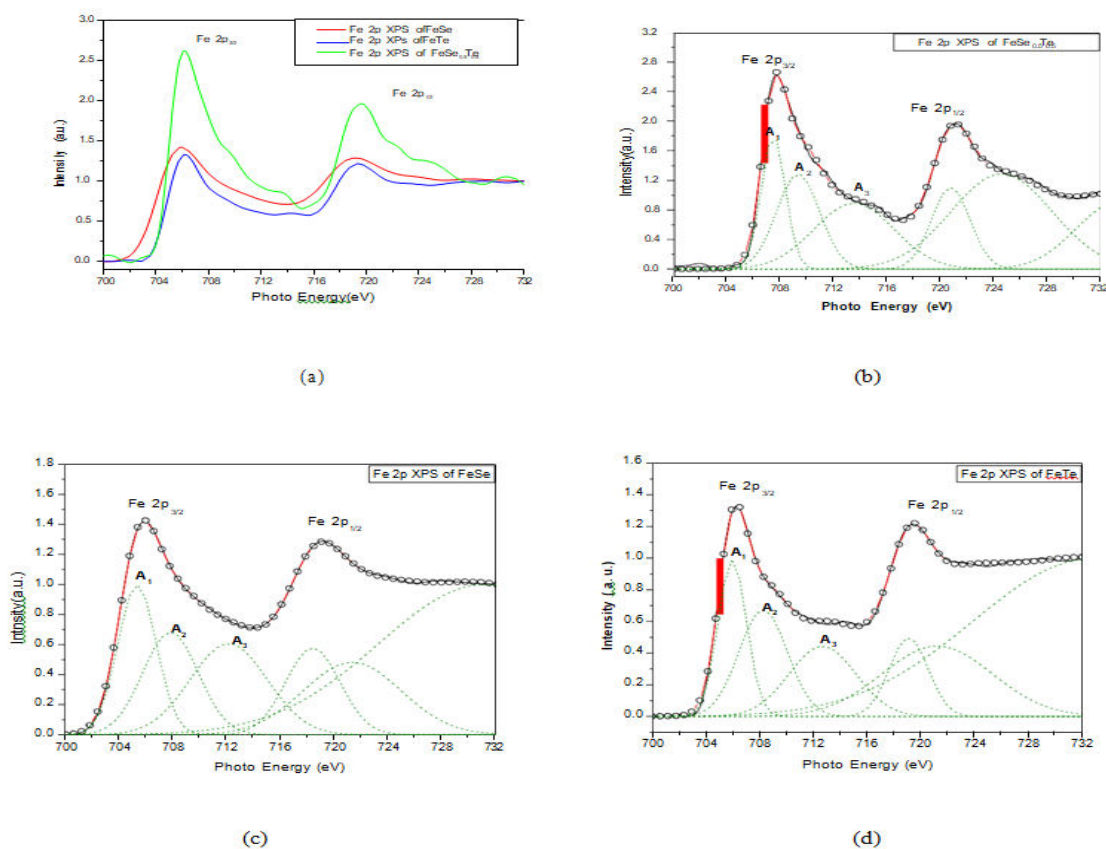


Figure 1: XPS core level spectra of Fe 2p showing (a) combined spectra of all samples (b) for FeSe_{0.5}Te_{0.5} sample, (c) for FeSe sample, and (d) for FeTe sample. There is shift of ~0.05eV towards the high energy side with Te/Se doping for the Fe 2p core level.

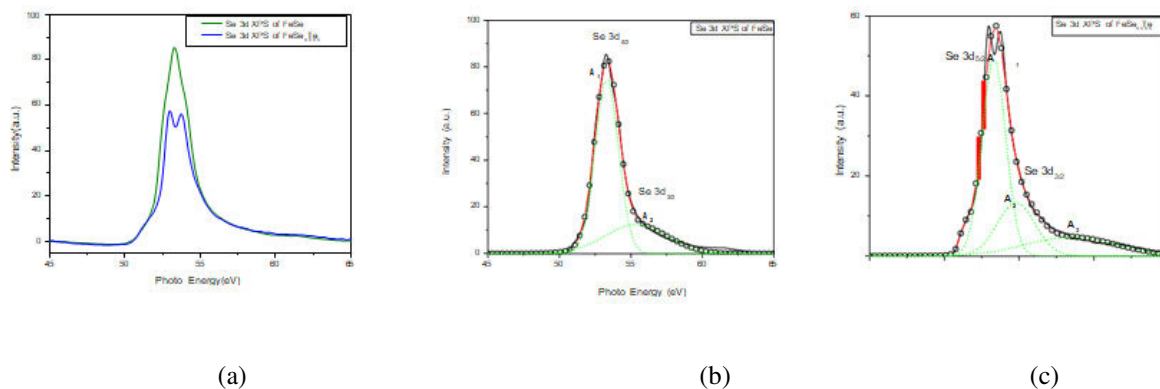


Figure 2: XPS core level spectra of Se 3d showing (a) combined spectra (b) for FeSe sample and (c) for FeSe_{0.5}Te_{0.5} sample.

With Te doping, the core level shifts up by ~0.062eV.

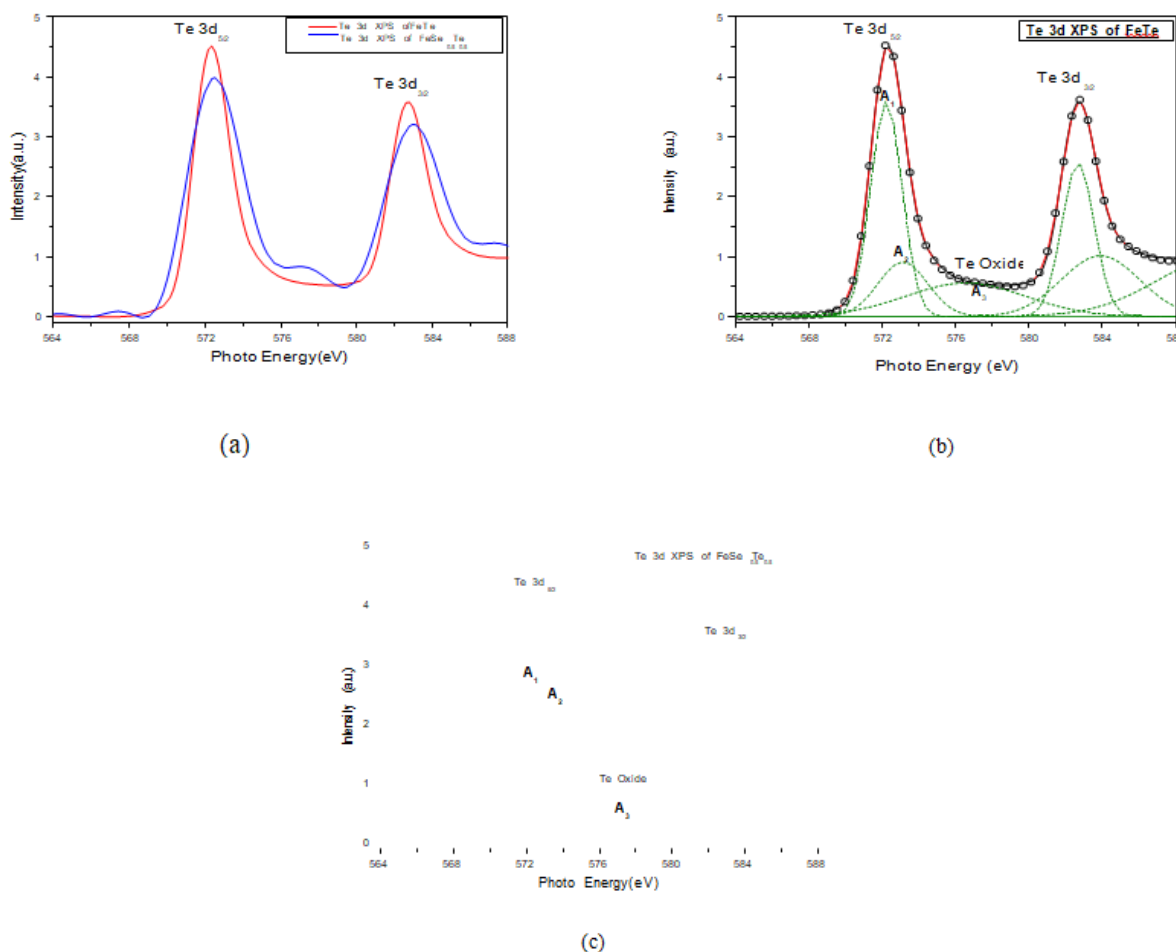


Figure 3: Core level spectrum of Te 3d showing (a) combined spectra of Te 3d samples (b) for FeTe sample and (c) for FeSe_{0.5}Te_{0.5} Sample is measured by X- ray photoelectron spectroscopy. With Te doping, the core level shifts up by 0.267eV.



INNO SPACE
SJIF Scientific Journal Impact Factor
Impact Factor:
5.928

ISSN

INTERNATIONAL
STANDARD
SERIAL
NUMBER
INDIA



INTERNATIONAL JOURNAL OF MULTIDISCIPLINARY RESEARCH IN SCIENCE, ENGINEERING AND TECHNOLOGY



9710 583 466



9710 583 466



ijmrset@gmail.com

www.ijmrset.com